JACS
JOURNAL OF THE AMERICAN CHEMICAL SOCIETY
Communication
pubs.acs.org/JACS

# Chiral Structure of Thiolate-Protected 28-Gold-Atom Nanocluster Determined by X-ray Crystallography

Chenjie Zeng,[†] Tao Li,[‡] Anindita Das,[†] Nathaniel L. Rosi,[‡] and Rongchao Jin*,[†]

[†]Department of Chemistry, Carnegie Mellon University, Pittsburgh, Pennsylvania 15213, United States
[‡]Department of Chemistry, University of Pittsburgh, Pittsburgh, Pennsylvania 15213, United States

Supporting Information

**ABSTRACT:** We report the crystal structure of a new nanocluster formulated as $Au_{28}(TBBT)_{20}$, where TBBT = 4-*tert*-butylbenzenethiolate. It exhibits a rod-like $Au_{20}$ kernel consisting of two interpenetrating cuboctahedra. The kernel is protected by four dimeric "staples" (-SR-Au-SR-Au-SR-) and eight bridging thiolates (-SR-). The unit cell of $Au_{28}(TBBT)_{20}$ single crystals contains a pair of enantiomers. The origin of chirality is primarily rooted in the rotating arrangement of the four dimeric staples as well as the arrangement of the bridging thiolates (quasi-$D_2$ symmetry). The enantiomers were separated by chiral HPLC and characterized by circular dichroism spectroscopy.

In recent years, metal nanocluster research has emerged as a new frontier in nanoscience.[1] Understanding the evolution from the discrete electronic states in relatively small nanoclusters (e.g., comprising a dozen metal atoms) to the quasi-continuous electronic band in much larger metallic nanoparticles (e.g., comprising at least a few hundred atoms) requires the synthesis of atomically precise nanoclusters and determination of their atom-packing structures, not only of the metal core but also of the ligand binding modes.[2−6] Based upon the total structures of nanoclusters, fundamental understanding of the electronic structure, optical and chiroptical, and catalytic properties can be attained at a deep level.[7−17] In terms of the synthesis, a number of atomically precise gold and silver nanoclusters protected by thiolate ligands have been reported.[18−29] On the other hand, there has also been new progress in the synthesis and structure determination of phosphine or phosphine/thiolate protected metal nanoclusters.[30−35] For thiolate-capped nanoclusters, a size-focusing methodology has been established, which has been demonstrated to be quite universal in the synthesis of many gold nanoclusters.[36]

Our recent efforts focus on structural elucidation. Following the previous determination of $[Au_{25}(PET)_{18}]^{-1/0}$, where PET = $SCH_2CH_2Ph$), $[Au_{36}(TBBT)_{24}]^0$, where TBBT = SPh-*t*-Bu), and $[Au_{38}(PET)_{24}]^0$ structures,[4−6] herein we report a new thiolate-protected nanocluster formulated as $Au_{28}(TBBT)_{20}$ and its crystal structure determined by X-ray crystallography.

The $Au_{28}(TBBT)_{20}$ nanocluster was synthesized by reacting pure $[Au_{25}(PET)_{18}]^-TOA^+$, where TOA = $^+N(n\text{-}C_8H_{17})_4$, with excess TBBT thiol at 80 °C (details in Supporting Information (SI)). After ∼2 h, all the $Au_{25}(PET)_{18}$ nanoclusters were completely converted to $Au_{28}(TBBT)_{20}$ in high yield (>90%, Au atom basis); no byproducts were observed. The as-obtained nanoclusters were crystallized in mixed $CH_2Cl_2$ and ethanol (3:2, v). Rhombic brown crystals were observed after one day, and they were analyzed by single crystal X-ray crystallography.

The $Au_{28}(TBBT)_{20}$ nanoclusters crystallized in a triclinic $P\bar{1}$ space group. Interestingly, the unit cell comprises a pair of enantiomers (Figure 1), as in the cases of $Au_{102}(SR)_{44}$ and $Au_{38}(SR)_{24}$.[2,5] Below we choose the left-handed enantiomer for a detailed analysis of the structure.

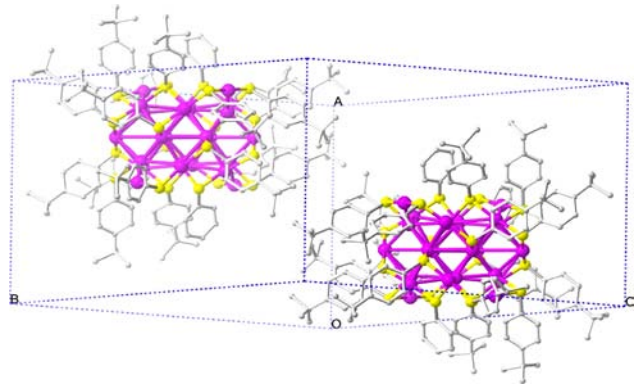


**Figure 1.** Total structure of the $Au_{28}(TBBT)_{20}$ nanocluster. The unit cell contains a pair of left- and right-handed isomers. Color labels: magenta = Au atoms; yellow = sulfur; gray = carbon.

The kernel of $Au_{28}(TBBT)_{20}$ is composed of two interpenetrating cuboctahedra, as shown in Figure 2. The two cuboctahedra share six common atoms (highlighted in green, Figure 2B), hence the kernel has 13 + 13 − 6 = 20 gold atoms; note that the cuboctahedra are slightly distorted (comparing Figure 2A,C). This rod-like $Au_{20}$ kernel can be viewed as a fragment of the face-centered cubic (fcc) structure adopted in bulk gold and nanoparticles typically >2 nm (diameter).[1d] Due to the fcc symmetry, the $Au_{20}$ kernel exhibits layer-by-layer atomic planes, and the planes of *a*-*b*-*c* can be indexed as {111} (Figure 2B). The surface of the $Au_{20}$ rod is enclosed by well-defined crystal planes, including four isosceles-trapezoid-shaped {111} facets on the front and back (Figure 2D, blue shadowed), two rectangular shaped {100} faces on the top and bottom (Figure 2D, yellow shadowed), and two square {100} and two

**Received:** April 23, 2013
**Published:** July 1, 2013

   dx.doi.org/10.1021/ja404058q | J. Am. Chem. Soc. 2013, 135, 10011−10013

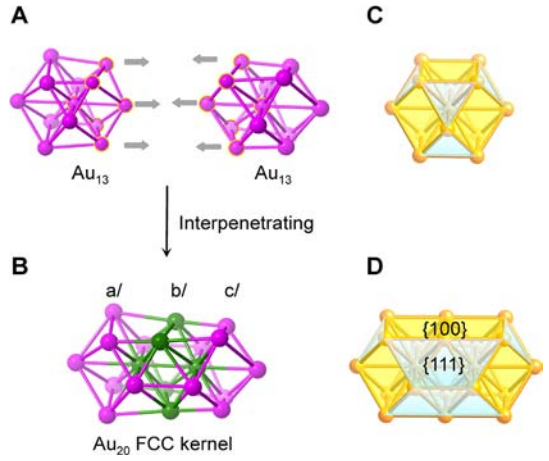


**Figure 2.** (A,B)The $Au_{20}$ kernel structure in $Au_{28}(TBBT)_{20}$; (C,D) models of cuboctahedron and interpenetrated bicuboctahedron.

triangle {111} facets on each end of the $Au_{20}$ rod (Figure 2D). The $Au_{20}$ kernel adopts a quasi-$D_{2h}$ symmetry.

Next we discuss the surface structure of $Au_{28}(TBBT)_{20}$. Four dimeric staples (-SR-Au-SR-Au-SR-) can be easily identified on the four {111} facets of the $Au_{20}$ kernel (Figure 3A): two facing

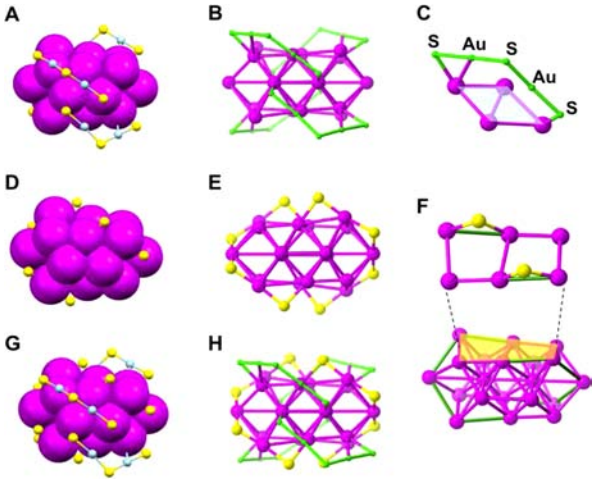


**Figure 3.** Thiolate-binding modes in $Au_{28}(TBBT)_{20}$: (A−C) Dimeric staples (total: four); (D−F) Bridging thiolates (total: eight); (G,H) Overall $Au_{28}S_{20}$ framework. (Magenta = Au atoms in the kernel; blue = Au in dimeric staples; yellow = sulfur; the four dimeric staples are highlighted in green in panels B, C, and H).

front and the other two facing back (Figure 3B). The two end-sulfur atoms of each dimeric staple bind to the two farthest Au atoms of a diamond-like unit (Figure 3C); the latter consists of two edge-shared triangles on the {111} facet. In addition to the four dimeric staples, we also found that the remaining eight thiolates simply bridge on the Au−Au edges of the {100} facets of the $Au_{20}$ kernel (Figure 3D−F). All eight bridging thiolates are nearly perpendicular to the underneath eight square faces (Figure 3F). The above anatomy of the $Au_{28}(SR)_{20}$ structure suggests that the nanocluster formula may be written as $Au_{20}[Au_2(SR)_3]_4(SR)_8$ to illustrate the $Au_{20}$ kernel, four $Au_2(SR)_3$ dimeric staples, and eight SR bridging thiolates. The arrangement of the dimeric staples and the bridging thiolates renders the $Au_{28}(SR)_{20}$ nanocluster an overall quasi-$D_2$ symmetry (Figure 3G,H), with the three mutually perpendicular 2-fold rotation axes ($x$, $y$, $z$) as indicated in Figure S1; therefore, the $Au_{28}(TBBT)_{20}$ structure is chiral.

The Au−Au bond length in the bicuboctahedral kernel is 2.99 (average) or 2.92 Å if excluding the particular Au−Au bonds (Figure 3F, green bonds) under the bridging thiolates, which are relatively longer (Figure S2). The 2.92 Å average distance is comparable to the 2.88 Å bond length in bulk gold. The Au−Au bonds under the eight bridging thiolates are somewhat stretched, with an average of 3.40 Å. This stretching effect contributes to the distortion of the bicuboctahedral kernel. On the other hand, the dimeric staple tends to clamp the underneath gold atoms together, giving rise to a shorter Au−Au bond length under the dimeric staple (Figure S2), with an average of 2.87 Å.

The Au−S bonds give an overall average of 2.31 Å (standard deviation: 0.04 Å), with no significant difference between the dimeric and bridging cases (2.31 vs 2.30 Å, respectively). The average Au−S−Au bond angle is 94.62° (standard deviation: 10.57°). The bond angle in the dimeric staples is more flexible, ranging from 75.5° to 106.34°, while in the bridging thiolate the value is from 87.32° to 108.07°. Of note, the average Au−Au and Au−S bond precision is ±0.0034 Å and ±0.0161 Å, respectively.

The chirality of $Au_{28}(TBBT)_{20}$ originates from the quasi-$D_2$ symmetry of the nanocluster. The two enantiomers are shown in Figure 4A. The chirality can be easily viewed from the left-

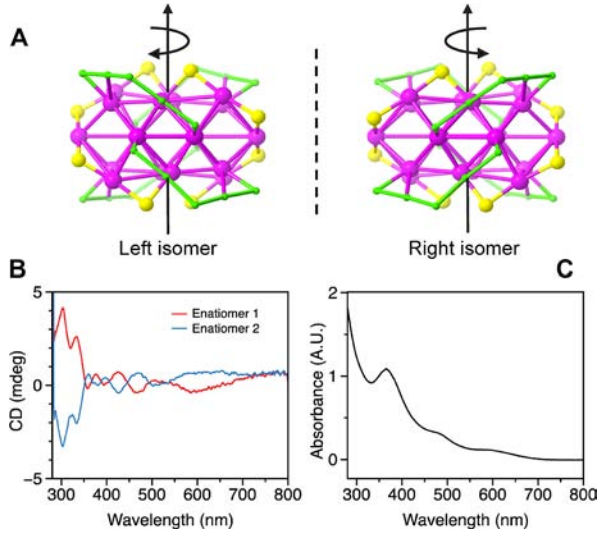


**Figure 4.** (A) The two enantiomers of $Au_{28}(TBBT)_{20}$. (B) CD spectra of enantiomer-1 and -2. (C) Normal optical absorption spectrum.

and right-handed arrangement of the dimeric staples (highlight in green in Figure 4A). We tentatively define the left and right isomers by the orientation of the dimeric staples on the {111} facets as indicated in Figure 4A. Of note, the bridging thiolates also impact chirality to the $Au_{28}$ clusters. We further used chiral-HPLC[15b] to separate the enantiomers (Figure S3, see the SI for details). The as-separated enantiomers were characterized by circular dichroism (CD) spectroscopy (Figure 4B). The mirror-imaged CD spectra exhibit two distinct bands at 300 and 340 nm, weak peaks at 360, 380, 400, 425, and 470 nm, and a broad peak at 600 nm. In contrast, the normal optical absorption spectrum of $Au_{28}(TBBT)_{20}$ only shows three stepwise peaks at 365, 480, and 580 nm (Figure 4C). By extrapolating the absorbance to zero, we determined the optical


dx.doi.org/10.1021/ja404058q | J. Am. Chem. Soc. 2013, 135, 10011−10013

bandgap to be ~1.78 eV, comparable to that of $Au_{36}(TBBT)_{24}$.[6] Future theoretical calculations may reveal insight into why $Au_{28}(TBBT)_{20}$ and $Au_{36}(TBBT)_{24}$ exhibit similar bandgaps.

The $Au_{28}(TBBT)_{20}$ nanocluster is charge neutral, as indicated by the absence of counterions in the unit cell and by the null signals in electrospray ionization mass spectrometric analysis (ESI-MS). Therefore, $Cs(OAc)_2$ was added to the nanocluster solution to form $Cs^+$ adducts for ESI-MS analysis in positive mode (Figure S4). The clean ESI mass spectrum confirms the purity of $Au_{28}(TBBT)_{20}$. Two peaks were observed at $m/z$ 8953.4 and 4542.6; note that the low mass end ($m/z$ < ~4700) shows uniformly spaced $[CsOAc]_xCs^+$ with 192 Da spacing (corresponding to the formula weight of CsOAc). The $m/z$ 4542.6 peak is 2+ charged, as revealed by the isotope peak spacing ($\delta$ = 0.5, Figure S4 inset), therefore the cluster mass is determined to be 8819.2 after subtracting two Cs+ ions. The $m/z$ 8953.4 peak is the monocation and gives the same cluster mass (8820.4 Da) after subtracting one $Cs^+$. The experimental mass matches perfectly with the calculated value of $Au_{28}(TBBT)_{20}$ (calcd: 8820.0 Da). Furthermore, the simulated isotope pattern also matches the experimental one (Figure S4, inset). Taken together, X-ray crystallography and ESI-MS analysis unambiguously establish the $Au_{28}(TBBT)_{20}$ formula and its molecular purity.

In summary, we have synthesized a new gold nanocluster formulated $[Au_{28}(TBBT)_{20}]^0$, and the crystal structure was solved by single crystal X-ray crystallography. The fcc kernel of this nanocluster constitutes the second example of ultrasmall fcc particles. The emergence of fcc structure in both $Au_{28}(TBBT)_{20}$ and $Au_{36}(TBBT)_{24}$ indicates the critical role of ligands in determining the structure and size. Future work will gain further insight into this intriguing issue.

## ■ ASSOCIATED CONTENT

### Supporting Information

Synthesis details and crystallization and X-ray analysis as well as Figures S1−4. This material is available free of charge via the Internet at http://pubs.acs.org.

## ■ AUTHOR INFORMATION


### Corresponding Author

rongchao@andrew.cmu.edu


### Notes

The authors declare no competing financial interest.

## ■ ACKNOWLEDGMENTS

The work is supported by the U.S. Department of Energy-Office of Basic Energy Sciences, grant DE-FG02-12ER16354. We thank Dr. Zhongrui Zhou for assistance in ESI-MS analysis and Dr. Huifeng Qian for valuable discussion.

## ■ REFERENCES


(1) (a) Jin, R. *Nanoscale* **2010**, *2*, 343. (b) Negishi, Y.; Nobusada, K.; Tsukuda, T. *J. Am. Chem. Soc.* **2005**, *127*, 5261. (c) Alvarez, M. M.; Khoury, J. T.; Schaaff, T. G.; Shafigullin, M. N.; Vezmar, I.; Whetten, R. L. *J. Phys. Chem. B* **1997**, *101*, 3706. (d) Qian, H.; Zhu, Y.; Jin, R. *Proc. Natl. Acad. Sci. U.S.A.* **2012**, *109*, 696. (e) Dass, A. *J. Am. Chem. Soc.* **2011**, *133*, 19259. (f) Pei, Y.; Zeng, X. C. *Nanoscale* **2012**, *4*, 4054.

(2) Jadzinsky, P. D.; Calero, G.; Ackerson, C. J.; Bushnell, D. A.; Kornberg, R. D. *Science* **2007**, *318*, 430.

(3) Heaven, M. W.; Dass, A.; White, P. S.; Holt, K. M.; Murray, R. W. *J. Am. Chem. Soc.* **2008**, *130*, 3754.

(4) (a) Zhu, M.; Aikens, C. M.; Hollander, F. J.; Schatz, G. C.; Jin, R. *J. Am. Chem. Soc.* **2008**, *130*, 5883−5885. (b) Zhu, M.; Eckenhoff, W. T.; Pintauer, T.; Jin, R. *J. Phys. Chem. C* **2008**, *112*, 14221.

(5) Qian, H.; Eckenhoff, W. T.; Zhu, Y.; Pintauer, T.; Jin, R. *J. Am. Chem. Soc.* **2010**, *132*, 8280.

(6) Zeng, C.; Qian, H.; Li, T.; Li, G.; Rosi, N. L.; Yoon, B.; Barnett, R. N.; Whetten, R. L.; Landman, U.; Jin, R. *Angew. Chem., Int. Ed.* **2012**, *51*, 13114.

(7) (a) Tsukuda, T. *Bull. Chem. Soc. Jpn.* **2012**, *85*, 151. (b) Qian, H.; Zhu, M.; Wu, Z.; Jin, R. *Acc. Chem. Res.* **2012**, *45*, 1470.

(8) Varnavski, O.; Ramakrishna, G.; Kim, J.; Lee, D.; Goodson, T. *J. Am. Chem. Soc.* **2010**, *132*, 16.

(9) Jiang, D.; Whetten, R. L. *Phys. Rev. B* **2009**, *80*, 115402.

(10) Qian, H.; Zhu, M.; Gayathri, C.; Gil, R. R.; Jin, R. *ACS Nano* **2011**, *5*, 8935.

(11) Schaaff, T. G.; Whetten, R. L. *J. Phys. Chem. B* **2000**, *104*, 2630.

(12) Yanagimoto, Y.; Negishi, Y.; Fujihara, H.; Tsukuda, T. *J. Phys. Chem. B* **2006**, *110*, 11611.

(13) Sánchez-Castillo, A.; Noguez, C.; Garzón, I. L. *J. Am. Chem. Soc.* **2010**, *132*, 1504.

(14) (a) Aikens, C. M. *J. Phys. Chem. Lett.* **2011**, *2*, 99. (b) Provorse, M. R.; Aikens, C. M. *J. Am. Chem. Soc.* **2010**, *132*, 1302.

(15) (a) Malola, S.; Lehtovaara, L.; Knoppe, S.; Hu, K.-J.; Palmer, R. E.; Bürgi, T.; Häkkinen, H. *J. Am. Chem. Soc.* **2012**, *134*, 19560. (b) Knoppe, S.; Dolamic, I.; Dass, A.; Bürgi, T. *J. Am. Chem. Soc.* **2012**, *134*, 20302. (c) Yao, H. *J. Phys. Chem. Lett.* **2012**, *3*, 1701.

(16) Zhu, M.; Qian, H.; Meng, X.; Jin, S.; Wu, Z.; Jin, R. *Nano Lett.* **2011**, *11*, 3963.

(17) Li, G.; Jin, R. *Acc. Chem. Res.* **2013**, DOI: 10.1021/ar300213z.

(18) Zhu, M.; Lanni, E.; Garg, N.; Bier, M. E.; Jin, R. *J. Am. Chem. Soc.* **2008**, *130*, 1138.

(19) Nishigaki, J.; Tsunoyama, R.; Tsunoyama, H.; Ichikuni, N.; Yamazoe, S.; Negishi, Y.; Ito, M.; Matsuo, T.; Tamao, K.; Tsukuda, T. *J. Am. Chem. Soc.* **2012**, *134*, 14295.

(20) Tracy, J. B.; Crowe, M. C.; Parker, J. F.; Hampe, O.; Fields-Zinna, C. A.; Dass, A.; Murray, R. W. *J. Am. Chem. Soc.* **2007**, *129*, 16209.

(21) Nimmala, P. R.; Yoon, B.; Whetten, R. L.; Landman, U.; Dass, A. *J. Phys. Chem. A* **2013**, *117*, 504.

(22) Heinecke, C. L.; Ni, T. W.; Malola, S.; Makinen, V.; Wong, O. A.; Hakkinen, H.; Ackerson, C. *J. Am. Chem. Soc.* **2012**, *134*, 13316.

(23) (a) Negishi, Y.; Sakamoto, C.; Ohyama, T.; Tsukuda, T. *J. Phys. Chem. Lett.* **2012**, *3*, 1624. (b) Qian, H.; Jin, R. *Nano Lett.* **2009**, *9*, 4083.

(24) (a) Yu, Y.; Luo, Z.; Yu, Y.; Lee, J. Y.; Xie, J. *ACS Nano* **2012**, *6*, 7920. (b) Habeeb Muhammed, M. A.; Pradeep, T. *Small* **2011**, *7*, 204.

(25) Guo, J.; Kumar, S.; Bolan, M.; Desireddy, A.; Bigioni, T. P.; Griffith, W. P. *Anal. Chem.* **2012**, *84*, 5304.

(26) Harkness, K. M.; Tang, Y.; Dass, A.; Pan, J.; Kothalawala, N.; Reddy, V. J.; Cliffel, D. E.; Demeler, B.; Stellacci, F.; Bakr, O. M.; McLean, J. A. *Nanoscale* **2012**, *4*, 4269.

(27) Cathcart, N.; Kitaev, V. *J. Phys. Chem. C* **2010**, *114*, 16010.

(28) Negishi, Y.; Arai, R.; Niihori, Y.; Tsukuda, T. *Chem. Commun.* **2011**, *47*, 5693.

(29) Udayabhaskararao, T.; Sun, Y.; Goswami, N.; Pal, S. K.; Balasubramanian, K.; Pradeep, T. *Angew. Chem., Int. Ed.* **2012**, *51*, 2155.

(30) Mednikov, E. G.; Dahl, L. F. *J. Am. Chem. Soc.* **2008**, *130*, 14813.

(31) Pettibone, J. M.; Hudgens, J. W. *ACS Nano* **2011**, *5*, 2989.

(32) (a) Wan, X.-K.; Lin, Z.-W.; Wang, Q.-M. *J. Am. Chem. Soc.* **2012**, *134*, 14750. (b) Das, A.; Li, T.; Nobusada, K.; Zeng, Q.; Rosi, N. L.; Jin, R. *J. Am. Chem. Soc.* **2012**, *134*, 20286.

(33) Shichibu, Y.; Konishi, K. *Small* **2010**, *6*, 1216.

(34) Shichibu, Y.; Negishi, Y.; Watanabe, T.; Chaki, N. K.; Kawaguchi, H.; Tsukuda, T. *J. Phys. Chem. C* **2007**, *111*, 7845.

(35) Yang, H.; Wang, Y.; Zheng, N. *Nanoscale* **2013**, *5*, 2674.

(36) Jin, R.; Qian, H.; Wu, Z.; Zhu, Y.; Zhu, M.; Mohanty, A.; Garg, N. *J. Phys. Chem. Lett.* **2010**, *1*, 2903.